Egypt. J. Chem. **Vol. 64,** No. 7 pp. 3873 - 3887 (2021)

Egyptian Journal of Chemistry

http://ejchem.journals.ekb.eg/

Modulation of cancer therapy using nano-organometallic compounds: preparation, spectroscopic characterization and cytotoxic evaluation

Abdou S. El-Tabl*[a], Moshira M. Abd-El Wahed[b], Eman A. Mohamed[a] , Mohammed H. H. Abu-Setta[a]

[a] *Department of Chemistry, Faculty of Science, Menoufia University, Shebin El -Kom, Egypt.*
[b] *Department of Pathology, Faculty of Medicine, Menoufia University, Shebin El-Kom, Egypt.*

Abstract

New series of Mn(II), Co(II), Ni(II), Cu(II), Zn(II) and Cd(II) organometallic complexes with hydroxyl benzylidene malonohydrazide ligand have much potential as therapeutic and diagnostic agents. The ligand allows the thermodynamic and kinetic reactivity of the metal ion to be controlled and also provide a scaffold for functionalization. The establishment of structure activity relationships and elucidation of the specification of complexes under conditions relevant to drug testing and formulation are crucial for the further development of promising medicinal applications of organometallic complexes. Specific examples involving the design of metal complexes as anticancer agents are discussed. These complexes have been synthesized and characterized by (^{1}H-NMR, mass, IR, UV-VIS and ESR) spectroscopy, as well as magnetic moments, conductance, elemental and thermal analyses. Molar conductance in DMF solution indicates that, the complexes are non-electrolytes. The ESR spectra of solid Cu(II) complexes **(7)** and **(8)** showed isotropic and anisotropic types indicating an octahedral geometry with covalent bond character. However, Co(II) complexes **(3)** and (4) showed anisotropic type where, $g_{\perp} > g_{\parallel} > 2.0023$, indicating compressed tetragonal distortion around Co(II) ion. Cytotoxic evolution of the ligand and its complexes have been carried out. Complexes showed enhanced activity in comparison to the parent ligand or standard drug applied

1. Introduction

Schiff-bases have played a key role in the development of coordination chemistry. Schiff- base compounds containing an imine group are usually formed by the condensation of a primary amines with an active carbonyl or aldehyde group. These compounds are considered as a very important class of organic compounds, which have wide applications in many biological spects[1].Various Schiff–bases complexes were reported to possess geno-toxicity[2,3], antibacterial[4,5] and antifungal activities[6]. The increasing interest in transition metal complexes containing Schiff-base ligand is derived from their well-established role in biological systems as well as their catalytic and pharmaceutical application[7]. Metal complexes provide a highly versatile platform for drug design. Besides variation in the metal and its oxidation state, that allow the fine-tuning of their chemical reactivity in terms of both kinetics and thermodynamics. Not only the metal but also the ligands can play important roles in biological activity, ranging from outer-sphere recognition of the target site to the activity of any released ligands and ligand centered redox processes. Due to a growing interest in the in the development of metallo-therapeutic drugs and metal-based agents[8, 9], we reported herein

*Corresponding author e-mail: asaeltabl@yahoo.com.
Receive Date: 21 February 2021, Revise Date: 21 March 2021, Accept Date: 28 March 2021
DOI: 10.21608/EJCHEM.2021.64313.3379

synthesis and characterization of new metallo-therapeutic candidates derived from the novel ligand (N'1E,N'3E)-N'1,N'3-bis (2-hydroxybenzylidene) malonohydrazide. The cytotoxic activity of synthesized compounds has been also investigated.

2. Experimental

Instrumentation and measurement:

The ligand and its complexes were synthetic grade and used without further purification. C, H, N and Cl analyses were determined at the Analytical Unit of Cairo University, Egypt. A standard gravimetric method was used to determine metal ions[10-12]. All metal complexes were dried under vacuum over P_4O_{10}. The IR spectra were measured as KBr pellets using a Perkin-Elmer 683 spectrophotometer (4000-400 cm-1). Electronic spectra (qualitative) were recorded on a Perkin-Elmer 550 spectrophotometer. The conductance(10^{-3}M) of the complexes in DMF were measured at 25 °C with a Bibby conduct meter type MCl. ^{1}H-NMR spectra of the ligand and its Cd(II) complex were obtained with Perkin-Elmer R32-90-MHz spectrophotometer using TMS as internal standard. Mass spectra were recorded using JEULJMS-AX-500 mass spectrometer provided with data sys-tem. The thermal analyses (DTA and TGA) were carried out in air on a Shimadzu DT-30 thermal analyzer from 27 to 800 °C at a heating rate of 10 °C per minute. Magnetic susceptibilities were measured at 25 °C by the Gouy method using mercuric tetrathiocyanatocobalt(II) as the magnetic susceptibility standard. Diamagnetic corrections were estimated from Pascal's constant[13].The magnetic moments were calculated from the equation: The ESR spectra of solid complexes at room temperature were recorded using a varian E-109 spectrophotometer, DPPH was used as a standard material. The TLC of all compounds confirmed their purity.

Transmission electron microscope (TEM): TEM samples for the colloidal suspensions of the complexes in dis.water were prepared by dropping the colloids onto carbon-coated TEM grids (Carbon coated Cu grids, Ted Pella, Redding, CA, USA) and allowing the liquid carrier to evaporate in air then assaying by a JEOL 1230 transmission electron microscope (120 kV).

BIOLOGICAL ACTIVITY

Cytotoxic activity: Evaluation of the cytotoxic activity of the ligand and some of its metal complexes was carried out in the Pathology Laboratory, Pathology Department, Faculty of Medicine, El-Menoufia University, Egypt. The evaluation process was carried out in vitro using the Sulfo-Rhodamine-B-stain (SRB) assay published method[14,15]. Cells were plated in 96-multiwell plate (10^4cells/well) for 24 hrs. Before treatment with the complexes to allow attachment of cell to the wall of the plate. Different concentrations of the compounds under test in DMSO (0, 5, 12.5, 25 and 50 µg/ml) were added to the cell monolayer, triplicate wells being prepared for each individual dose. Monolayer cells were incubated with the complexes for 48 hrs.at 37°C and using 5% CO_2. After 48 hrs.cells were fixed, washed and stained with Sulfo-Rhodamine-B-stain. Excess stain was wash with acetic acid and attached stain was recovered with Tris EDTA buffer. Color intensity was measured in an ELISA reader. The relation between surviving fraction and drug concentration is plotted to get the survival curve for each tumor cell line after addition the specified compound

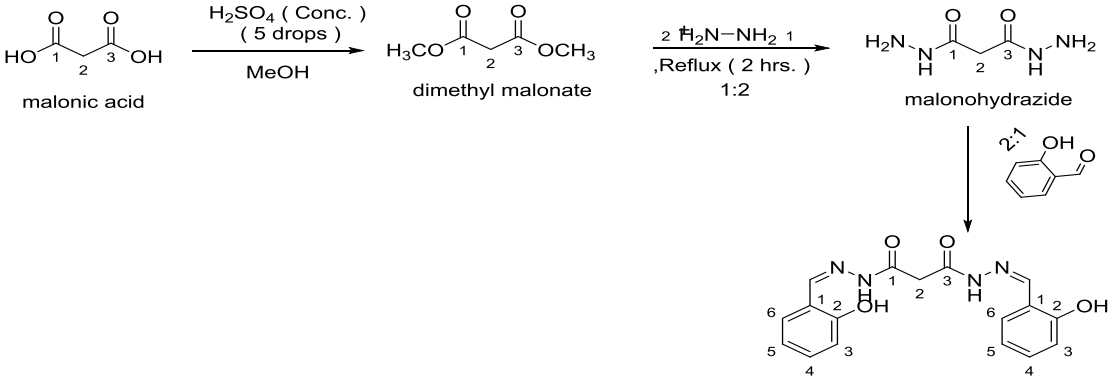

Scheme (1) Preparation of the ligand

Synthesis of metal complexes (2)-(13): The metal complexes **2-13** were prepared by refluxing with stirring a suitable amount of a hot ethanolic solution of the following metal salts: $Mn(OAc)_2 \cdot 4H_2O$, $Co(OAc)_2 \cdot 4H_2O$, $CoSO_4 \cdot 7H_2O$, $CoCl_2 \cdot 6H_2O$, $Ni(OAc)_2 \cdot 4H_2O$, $Cu(OAc)_2(H_2O)_2$, $CuSO_4.5H_2O$, $CuCl_2 \cdot 2H_2O$, $Cu(NO_3)_2 \cdot 2H_2O$, $CuCO_3$, $Zn(OAc)_2$. $2H_2O$, $Cd(OAc)_2.2H_2O$ and then added to hot ethanolic solution of the ligand with molar ratio (2 metal: 1 ligand). The refluxing times variedfrom 2 to 4 hours according to the depending to nature of metal ion. The precipitates which formed were filtered off, washed with ethanol then by diethyl ether and dried in vacuum desiccators over P_4O_{10}. Structure representation and analytical data for the prepared complexes are shown in figures 1 and 2 table 1.

3. Results and Discussion

All the metal complexes are stable at room temperature, no hydroscopic, insoluble in water, partially soluble in MeOH, EtOH, $CHCl_3$ and $(CH_3)_2CO$ and completely soluble in DMF and DMSO. The analytical and physical data, spectral data are compatible with the proposed structures, figure 1 and 2. The molar conductance of the complexes in 10^{-3} M DMF at 25 ^oC are in the 4.77-1.09 $ohm^{-1}cm^2mol^{-1}$ range, indicating a non-electrolytic nature[16]. These low values commensurate the absence of any counter ions in their structure[17]. Many attempts were made to grow a single
crystal but unfortunately, they were failed. Reaction of the ligand **(1)** with metal salts using (1L: 2M) molar ratio in ethanol gives complexes **(2)-(13).**

Table 1:-Analytical and Physical Data of the Ligand [H2L] (1) and its Metal Complexes.

No.	Ligand/Complexes	Color	FW	M.P (OC)	Yield (%)	Anal. /Found (Calc.) (%)					Molar conductance*
						C	H	N	M	Cl	
(1)	$[H_2L]$ $C_{17}H_{16}N_4O_4$	Reddish brown	340.33	>300	75	59.99(59.52)	4.74(4.61)	16.46(16.11)	-	-	
(2)	$[(H_2L)(Mn)_2(OAc)_4(H_2O)2] . 2H_2O$ $C_{25}H_{36}Mn_2N_4O_{16}$	Pale brown	722.42	>300	60	41.56(41.1)	4.46(4.23)	7.76(7.52)	15.21(14.98)	-	4.52
(3)	$[(H_2L)(Co)_2(OAc)_4(H_2O)2] . H_2O$ $C_{25}H_{34}Co_2N_4O_{15}$	Gray	730.41	>300	65	41.11(40.95)	4.42(4.0)	7.67(7.23)	16.14(15.98)	-	1.24
(4)	$[(H_2L)(Co)_2(SO_4)_2(H_2O)_4] . 2H_2O$ $C_{17}H_{28}Co_2N_4O_{18}S_2$	Yellowish brown	722.39	>300	70	28.26(27.92)	3.35(3.01)	7.76(7.43)	16.32(16.01)	-	1.09
(5)	$[(H_2L)(Co)_2(Cl)_4(H_2O)_2] . H_2O$ $C_{17}H_{22}Cl_4Co_2N_4O_7$	Dark brown	636.04	>300	73	32.10(31.87)	3.17(2.98)	8.81(8.55)	18.53(18.21)	22.30(21.89	2.64
(6)	$[(H_2L)(Ni)_2(OAc)_4(H_2O)_2] . 3H_2O$ $C_{25}H_{38}N_4Ni_2O_{17}$	Brown	729.93	>300	80	41.14(40.89)	4.31(4.42)	7.68 (7.25)	16.08I(15.93)	-	4.77
(7)	$[(H_2L)(Cu)_2(OAc)_4(H_2O)2] . H_2O$ $C_{25}H_{34}Cu_2N_4O_{15}$	Rose	737.62	>300	70	40.71(40.32)	4.42(4.31)	7.60(7.45)	17.23(16.89)	-	2.15
(8)	$[(H_2L)(Cu)_2(SO_4)_2(H_2O)_4] . H_2O$ $C_{17}H_{26}Cu_2N_4O_{17}S_2$	Gray	731.61	>300	85	27.91(27.59)	3.31(3.11)	7.66(7.43)	17.37(17.01)	-	4.45
(9)	$[(H_2L)(Cu)_2(Cl)_4(H_2O)_2] . H_2O$ $C_{17}H_{22}Cl_4Cu_2N_4O_7$	Greenish yellow	645.27	>300	69	31.64(31.25)	3.12(2.98)	8.68(8.51)	19.70(19.49)	21.98(21.27)	4.97
(10)	$[(H_2L)(Cu)_2(NO_3)_4(H_2O)_2] . H_2O$ $C_{17}H_{22}Cu_2N_8O_{19}$	Greenish brown	751.48	>300	68	27.17(26.95)	2.68(2.32)	14.91(14.57)	16.91(16.71)	-	1.11
(11)	$[(H_2L)(Cu)_2(CO_3)_2(H_2O)_4] . H_2O$ $C_{21}H_{26}Cu_2N_4O_{15}$	Green	743.52	>300	75	33.92(33.81)	2.71(2.56)	7.54(7.13)	17.09(16.89)	-	1.49
(12)	$[(H_2L)(Zn)_2(OAc)_4(H_2O)_2] . H_2O$ $C_{25}H_{34}N_4O_{15}Zn_2$	Dark green	743.30	>300	69	40.40(40.20)	4.34(4.11)	7.54(7.34)	17.59(17.27)	-	3.87
(13)	$[(H_2L)(Cd)_2(OAc)_4(H_2O)_2] . 2H_2O$ $C_{25}H_{36}Cd_2N_4O_{16}$	Pale brown	837.36	>300	75	35.86(35.61)	3.85(3.55)	6.69(6.41)	26.85(26.59)	-	2.49

* Λm (Ω^{-1} cm^2 mol^{-1})

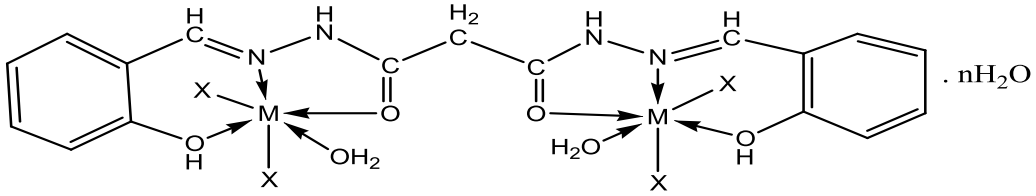

$[M(H_2L)(X_2)(H_2O)].nH_2O$

M= Mn(II), X= OAc, n= 2	**(2)**
M= Co(II), X= OAc, n= 1	**(3)**
M= Co(II), X= Cl, n= 1	**(5)**
M= Ni(II), X= OAc, n= 3	**(6)**
M= Cu(II), X= OAc, n= 1	**(7)**
M= Cu(II), X= Cl, n= 1	**(9)**
M= Cu(II), X= NO_3, n= 1	**(10)**
M= Zn(II), X= OAc, n= 1	**(12)**
M= Cd(II), X= OAc, n= 2	**(13)**

Fig. 1: Structure representation of complexes **(2), (3), (5-7), (9), (10), (12)** and **(13)**

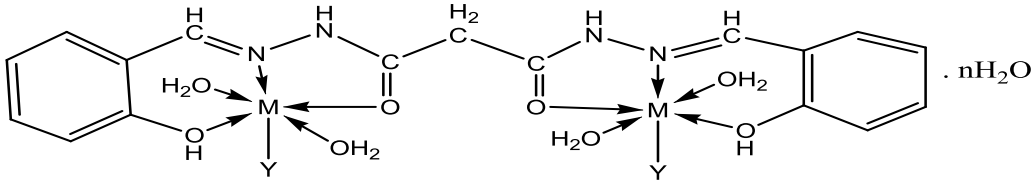

$[M(H_2L)(Y)(H_2O)_2].nH_2O$

M= Co(II), Y= SO_4, n= 2	**(4)**
M= Cu(II), Y= SO_4, n= 1	**(8)**
M= Cu(II), Y= CO_3, n= 1	**(11)**

Fig. 2: Structure representation of complexes **(4), (8)** and **(11)**

^{1}H-NMR spectra of the ligand (1) and and Zn(II) complex (12) : The ^{1}H-NMR spectra of ligand and Zn(II) complex (**12**) in deutrated DMSO showed peaks consistent with the proposed structure

(Scheme 1 and Figure 2). The ^{1}H-NMR spectrum of the ligand showed chemical shift observed as singlet at 9.96 ppm (s, 2H, OH[19,25]) which is assigned to proton of aromatic hydroxyl group. The chemical shifts which appeared at 8.8-8.9 ppm range was attributed to the azomethine protons ([12,17]H-C=N). However, the chemical shifts appeared as a singlet at 6.95 ppm is attributed to the proton of NH attached to carbonyl group. A set of signals appeared as multiples in the 7.09-7.3 ppm range, corresponding to protons of aromatic ring[17]. By comparison the ^{1}H NMR of the ligand and the spectrum of the Zn(II) complex **(12)**,

presence of the signal characteristic to the O*H* group appeared at 10.3 ppm indicating that the ligand bonded with the Zn(II) ions in its protonated form. In addition, there is a significant downfield shift of the azomethine proton signal and one from NH groups attached to carbonyl group relative to the free ligand clarified that the metal ions are coordinated to the azomethine nitrogen atom and NH nitrogen atom. This shift may be due to the formation of a coordination bond (N→Zn) [16,17].

Mass spectra: The mass spectra of (**1**) and its, Cu(II) complex, (**9**) confirmed their proposed formulation. The spectrum of (**1**) reveals the molecular ion peak (m ⁄z) at 340 amu consistent with the molecular weight of the ligand. Furthermore, the fragments observed at (m⁄z) = 59, 72, 90, 140, 170 and 338 amu correspond to C_4H_{11}, C_5H_{12}, $C_5H_{14}O$, $C_8H_{14}NO$, $C_8H_{14}N_2O_2$ and $C_{17}H_{14}N_4O_4$ moieties respectively. Complex (**9**) showed fragments (m⁄z) at 60, 72, 84, 130, 240 and 379 amu due to C_4H_{12}, C_5H_{12}, C_6H_{12}, $C_7H_{16}NO$, $C_{13}H_{19}ClNO$ and $C_{16}H_{12}ClCuN_2O_3$ moieties respectively.

IR Spectra:- The mode of bonding between the ligand and the metal ion revealed by comparing the IR spectra of the ligand (**1**) and its metal complexes (**2**)-(**13**) as shown in table 2. The ligand showed bands in the 3660-3345 and 3340-2680 cm^{-1} ranges, commensurate the presence of two types of intra- and intermolecular hydrogen bonds of OH and NH groups with imine group[26]. Thus, the higher frequency band is associated with a weaker hydrogen bond. The medium band at 3190 cm^{-1} is assigned to ν(NH) groups[18,19]. The ν(NH) group in the complexes appeared nearly at the same region of the free ligand indicating that, the NH group is not involved in the coordination to the metal ion[20]. However, the characteristic bands of imines, υ(C═N), υ(C═O) and υ(C-OH) were observed at 1662, 1735 cm^{-1} respectively. Strong band appeared at 1330-1240 cm^{-1} range is attributed to the υ(C-OH) vibration. The bands appeared at 1572-1458 and 780-750 cm^{-1} range, are assigned to υ(Ar) vibration[20, 21]. The υ(N-N) group appears at 1043 cm^{-1}. By comparing the IR spectra of the complexes (**2**)-(**13**) with that of the free ligand. It was found that, the position of the υ(C═N) bands of imines is shifted by 8-42 cm^{-1} range towards lower wave number in the complexes indicating coordination through nitrogen of azomethine group (CH═N)[20,21]. This is also confirmed by the appearance of new bands in the 586-516 cm^{-1} range, this has been assigned to the υ(M-N)[21]. Complexes (**2**)- (**13**) showed υ(C-OH) in the 1385-1149 range, indicating coordination to the metal ion[22].. The aromatic ring to the metal ion appeared in the 1575-1455 cm^{-1} and 870-740 cm^{-1} ranges[24].The IR spectra of the metal complexes (**2**)-(**19**) showed bands in the 3650-3610 cm^{-1}, 3360-3230 cm^{-1}, 3350-3210 cm^{-1} and 2875-2550 cm^{-1} ranges, commensurate the presence of two types of intra-and intermolecular hydrogen bonds. In acetate complexes, the acetate ion may be coordinate to the metal ion in unidentate, bidentate or bridging bidentate manner. The $\upsilon_{as}(CO_2)$ and $\upsilon_s(CO_2)$ of the free acetate ion are ca. 1560 and 1416 cm^{-1} respectively. In unidentate acetate complexes υ(C=O) is higher than $\upsilon_s(CO_2)$ and υ(C-O) is lower than $\upsilon_{as}(CO^{2-})$. As a result the separation between the two υ(CO) is much larger in unidentate than in free ion but in bidentate the separation is lower than in the free ion while in bridging bidentate the two υ(CO) is closer to the free ion[23]. In the case of acetate complexes (**2**), (**3**), (**6**), (**7**), (**12**) and (**13**) showed bands in the 1480-1430 and 1360-1326 cm^{-1} ranges, assigned to the asymmetric and symmetric stretches of the COO group. The mode of coordination of acetate group has often been deduced from the magnitude of the observed separation between the $\upsilon_{asym.}(COO^-)$ and $\upsilon_{sym.}(COO^-)$. The separation value (Δ) between $\upsilon_{asym}(COO^-)$ and $\upsilon_{sym.}(COO^-)$ in this complex was in the 120-104 cm^{-1} range suggesting the coordination of acetate group in these complexes as a monodentate fashion[18,23]. The sulphato complex (**4**) showed bands at 1285, 1180, 1041 and 740 cm^{-1} and complex (**8**) showed bands at 1252, 1167, 1082 and 750 cm^{-1} which assigned to monodentatesulphate group[24]. Complexes (**2**)-(**13**) showed bands in the 586-516 cm^{-1} is assigned to υ(M-N)[23]. Complexes (**2**)-(**13**) showed bands in the 678-612 cm^{-1} are due to υ(M-O)[25].

Table 2:-IR Frequencies of the Bands (cm^{-1}) of the Ligand [H_2L], (1) and its Metal complexes:

No.	ν(H_2O)	ν(OH)	υ(H-bonding)	ν(C=N)	ν(C=O)	ν(NH)	ν(COH)	ν(Ar)	ν(OAc /SO_4 /NO_3)	υ(M-O)	υ(M-N)	υ(M-Cl)
(1)	-	3470,3374	3660-3345, 3340-2680	1662	1735	3190	1330,1240	1572,783 1485,750	-	-	-	-
(2)	3568,3460-3332, 2986	3413,3366	3630-3288, 3210-2774	1620	1795,	3180	1385,1149	1571,1484 781,749	1448,1326	678	562*	-
(3)	3560,3340-3255, 3199	3423,3375	3640-3320, 3310-2773	1658	1725	3167	1320,1150	1530.1455 824,752	1430,1330	640	577	
(4)	3340, 3270-3095	3453	3630-3330, 3280-2860	1655	1733	3174	\1319,1190	1532,750 1575,827	1285,1180 1041,740	637	583	-
(5)	3450,3320-3316, 3002	3430,3379	3620-3230, 3210-2720	1650	1728	3160	1318,1194	1474,1532 858,826	-	650	582	450
(6)	3570,3360-3144, 3120	3430,3380	3620-3280, 3260-2550	1657	1725	3175	1283,1189	1477,1535 830,740	1450,1345	618	580	-
(7)	3560,3370-3325, 2945	3410,3380	3630-3320, 3300-2679	1670	1733	3150	1280,1185	1450,1575, 870	1450,1345	612	582	-
(8)	3570, 3365-3364, 3325	3433,3370	3650-3260, 3250-2663	1660	1730	3160	1310,1190	1575,1533 857,830	1252,1167 1082,750	615	586	-
(9)	3430,3550-3270, 3220	3427,3370	3610-3290, 3280-2784	1658	1732	3155	1310,1191	1575,1533 857,820	-	640	580	440
(10)	3428,3320-3200 3060	3432,3390	3650-3330, 3320-2867	1655	1728	3177	1315,1170	1570,1530 850,750	1339,1280,850	641	516	
(11)	3408,3230-3210, 3080	3432	3650-3330, 3320-2875	1654	1729	3150	1310,1220	1571,825 1538,760	1587,1360, 1070,750	640	520	-
(12)	3431,3260-3360, 3110	3420,3390	3640-3350, 3320-2870	1655	1730	3160	1275,1180	1565,1528 850,770	1480,1360	638	524	-
(13)	3455,3430-3350, 2750	3425,3383	3620-3360, 3350-2750	1656	1727	3165	1270,1170	1560,1532 840,765	1470,1345	630	537	-

Magnetic moments: The magnetic moments of the metal complexes (**2**)-(**13**) at room temperatures are shown in (Table 3). Copper(II) complexes (**7**) and (**11**) show values between 1.67 – 1.70 B.M, corresponding to one unpaired electron in an octahedral structure[26,27]. Cobalt(II) complexes (**3**), (**4**) and (**5**) showed values 4.38,4.85 and 4.42 B.M, indicating high spin octahedral cobalt(II) complexes[29,30] . Nickel(II) complex **(6)** showed 3.02 B.M, indicating octahedral Ni(II) complex[29,30]. Manganese (II) complex **(2)** gave 6.3 B.M, indicating high spin Mn(II) octahedral structure[29]. Zn(II) complex **(12)** and Cd(II) complex **(13)** showed diamagnetic property[30] .

Electronic spectra and magnetic moments: The electronic spectral data for the ligand (**1**) and its metal complexes in DMF solution are summarized in (Table 3). Ligand (**1**) in DMF solution showed two bands at 320 nm (ε =7.72 x 10^{-3} mol^{-1} cm^{-1}) and 295 nm (ε = 7.12x 10^{-3} mol^{-1} cm^{-1}) which may be assigned to n→π* and π→π* transitions of the imine and aromatic ring respectively[28]. Cobalt(II) complexes (**3**) ,(**4**) and (**5**) showed bands in the

290-292, 310-316, 460-495, 540-570 and 605-610 nm, the first two bands are within the ligand and the other bands are assigned to $^4T_{1g}(F)\rightarrow{}^4T_{2g}(P)(\nu_3)$, $^4T_{1g}(F)\rightarrow{}^4A_{2g}(\nu_2)$ and $^4T_{1g}(F)$ $^4T_{2g}(F)(\nu_1)$ transitions respectively indicating a compressed distorted tetragonal Co(II) complex the ν_2/ν_1 for the complexes are in the range 1.09-1.24 which is lower than the usual value 1.5, indicating distorted octahedral Co(II) complexes[31,33] . However, copper(II) complexes (**7**) and (**11**) showed bands in the 285-290 and 310-315 nm ranges , these bands are due to intraligand transitions, however, the bands appeared in the 440-462, 579-592 and 610-620 nm ranges, are assigned to O→Cu, charge transfer, $^2B^1\rightarrow{}^2E$ and $^2B_1\rightarrow{}^2B_2$ transitions, indicating a distorted tetragonal octahedral structure[31,32]. Manganese (II) complex **(3)** showed bands at 290,315, 425, 562 and 605 nm, the first bands are due to intraligand transitions and other bands are corresponding to $^6A_{1g}\rightarrow{}^4T_{4g}$, $^6A_{1g}\rightarrow{}^4E_g$ and $^6A_{1g}\rightarrow{}^4E_g$ transition respectively and compatible with an distorted octahedral geometry around Mn(II) ion[33]. Ni(II) complex **(6)** showed bands at 292, 316, 480, 575, 607 and 745 nm, the first two bands are due to intraligand transitions and the other bands are assigned to $^3A_{2g}(F)\rightarrow{}^3T_{2g}(F)(\nu_1)$,$^3A_{2g}(F)\rightarrow{}^3T_{1g}(\nu_2)$ and $^3A_{2g}(F)\rightarrow{}^3T_{1g}(P)(\nu_3)$ transitions respectively, which are consistent with distorted octahedral structure [33] . The ν_2/ν_1 for the complex is 1.19, confirming distorted octahedral structure. However, Zn(II) complex **(12)** and Cd(II) complex **(13)** showed bands at 292,318 and 293,320 and 325 nm respectively are due to intraligand transitions[31,32]**.**

Table (3): The electronic spectra (nm) and magnetic moments (B.M.) for the ligand (1), and its complexes

No.	Ligand/Complexes	λ_{max} (nm)	μ_{eff} (BM)	ν_2/ν_1
(1)	[HL]	295 nm (ε = 7.12x 10^{-3} mol^{-1} cm^{-1}) 320 nm (ε= 7.72 x 10^{-3} mol^{-1} cm^{-1})	-	-
(2)	$[(H_2L)(Mn)_2(OAc)_4(H_2O)_2]\cdot 2H_2O$	290,315,425,562,605	6.3	-
(3)	$[(H_2L)(Co)_2(OAc)_4(H_2O)_2]\cdot H_2O$	292,310,460,570,610	4.38	1.24
(4)	$[(H_2L)(Co)_2(SO4)_2(H_2O)_4]\cdot 2H_2O$	293,315,472,557,608	4.85	1.18
(5)	$[(H_2L)(Co)_2(Cl)_4(H_2O)_2]\cdot H_2O$	290,310,495,540,600	4.42	1.09
(6)	$[(H_2L)(Ni)_2(OAc)_4(H_2O)_2]\cdot 3H_2O$	292,316,480,575,607,745	3.02	1.19
(7)	$[(H_2L)(Cu)_2(OAc)_4(H_2O)_2]$.	285,310,440,585,620	1.67	-
(8)	$[(H_2L)(Cu)_2(SO_4)_2(H_2O)_4]\cdot H_2O$	289,312,452,592,615	1.69	-
(9)	$[(H_2L)(Cu)_2(Cl)_4(H_2O)_2]\cdot H_2O$	290,315,462,582,612	1.67	-
(10)	$[(H_2L)(Cu)_2(NO_3)_4(H_2O)_2]\cdot H_2O$	290,313,458,579,610	1.69	-
(11)	$[(H_2L)(Cu)_2(CO_3)_4(H_2O)_2]\cdot 2H_2O$	280,315,450,565,620	1.70	-
(12)	$[(H_2L)(Zn)_2(OAc)_4(H_2O)_2]\cdot H_2O$	292,318,322	Diamag.	-
(13)	$[(H_2L)(Cd)_2(OAc)_4(H_2O)_2]\cdot 2H_2O$	293,320,325	Diamag.	-

Electron spin resonance (ESR)

The ESR spectral data for complexes **(2), (3), (4), (5), (7)** and **(8), (9), (10), (11)** are presented in (Table 4). The spectra of Co(II) complexes **(3)**, **(4)** and **(5)** showed anisotropic and isotropic type where, $g_\perp > g_\parallel > 2.0023$, indicating compressed tetragonal distortion around Co(II) ion. However, complex **(5)** showed isotropic type with g_{iso} = 2.04. The spectra of copper(II) complexes **(8)** and **(11)** are characteristic of species d^9 configuration having axial type of a $d_{(x2-y2)}$ ground state which is the most common for copper(II) complexes[34,35]. The complexes showed $g_\parallel > g_\perp > 2.0023$, indicating distorted

octahedral geometry around copper(II) ion[36,37].The g-values are related by the expression G = ($g_{\|}$-2)/ ($g_{\perp}$ - 2)[36,38], where (G) exchange coupling interaction parameter (G). If G<4.0, a significant exchange coupling is present, whereas if G value > 4.0, local tetragonal axes are aligned parallel or only slightly misaligned. Complexes showed values indicating spin-exchange interactions take place between copper(II) ions. This phenomena is further confirmed by the magnetic moments values (Table 3). On the other hand, complex (**7**) showed isotropic type with g_{iso}= 2.15 indicating tetragonal axes are present in this complex. The $g_{\|}/A_{\|}$ value is also considered as a diagnostic term for stereochemistry[39], the $g_{\|}/A_{\|}$ values in the (105-135 cm^{-1}) range are expected for copper complexes within perfectly square planar geometry and for tetragonal distorted octahedral complexes are 150-250 cm^{-1}. The $g_{\|}/A_{\|}$ values for the copper complexes are 150.2, 181.1, 220 and 222 cm^{-1} which lie just within the range expected for the tetragonal distorted octahedral copper(II) complexes (Table 4). The g-value of the copper(II) complexes with a $^2B_{1g}$ ground state ($g_{\|}>g_{\perp}$) may be expressed by[40].

$$g_{|}=2.002–(8K^2_{\|}\lambda°/\Delta E_{xy}) \quad (1)$$

$$g_{\perp}=2.002–(2K^2_{\perp}\lambda°/\Delta E_{xz}) \quad (2)$$

Where $k_{\|}$ and $k_{\perp}$ are the parallel and perpendicular components respectively of the orbital reduction factor (K), $\lambda°$ is the spin-orbit coupling constant for the free copper, ΔE_{xy} and ΔE_{xz} are the electron transition energies of $^2B_{1g}\rightarrow{}^2B_{2g}$ and $^2B_{1g}\rightarrow{}^2E_g$. From the above relations, the orbital reduction factors ($K_{\|}$, $K_{\perp}$, K), which are measure terms for covalency[41], can be calculated. For an ionic environment, K=1; while for a covalent environment, K<1. The lower the value of K, the greater is the covalency.

$$K^2_{\perp} = (g_{\perp}- 2.002)\ \Delta E_{xz}/2\lambda_o \quad (3)$$

$$K^2_{\|} = (g_{\|} - 2.002)\ \Delta E_{xy}/8\lambda_o \quad (4)$$

$$K^2=(K_{2\|}+2K^2_{\perp})/3 \quad (5)$$

K values (Table 4), for the copper(II) complexes (**8**) - (**11**) are indicating for a covalent bond character[30,42]. Kivelson and Neiman noted that, for ionic environment $g_{\|}\geq 2.3$ and for a covalent environment $g_{\|}<2.3$[43]. Theoretical work by Smith[58] seems to confirmed this view. The g-values reported here (Table 4) show considerable covalent bond character[30]. Also, the in-plane σ-covalency parameter, α^2(Cu) was calculated by

$$\alpha^2(Cu)=(A_{\|}/0.036)+(g_{\|}-2.002)+3/7(g-2.002)+0.04 \quad (6)$$

The calculated values (Table 4) suggested a covalent bonding[30,42]. The in-plane and out of- plane π- bonding coefficients β_1^2 and β^2 respectively, are dependent upon the values of ΔE_{xy} and ΔE_{xz} in the following equations[43].

$$\alpha^2\beta^2 = (g_{\perp}- 2.002)\ \Delta E_{xy}/2\lambda_o \quad (7)$$

$$\alpha^2\beta_1^2 = (g_{\|} - 2.002)\ \Delta E_{xz}/8\lambda_o \quad (8)$$

In this work, complexes showed β_1^2 values 0.9, 0.8 and 0.93 indicating a moderate degree of covalency in the in-plane π-bonding[42,44]. β^2 value for complexes showed 1.79, 1.08,1.6 and 1.13 indicating ionic character of the out-of-plane. It is possible to calculate approximate orbital populations ford orbitals[45] by

$$A_{\|} = A_{iso} – 2B[1 \pm (7/4)\ \Delta g_{\|}]\ \ \Delta g_{\|}= g_{\|}- g_e \quad (9)$$

$$\alpha_{p,d}{}^2 =2B/\ 2B° \quad (10)$$

Where A° and 2B° is the calculated dipolar coupling for unit occupancy of d orbital respectively. When the data are analyzed, the components of the ^{45}Cu hyperfine coupling were considered with all the sign combinations. The only physically meaningful results are found when $A_{\|}$and $A_{\perp}$ were negative. The resulting isotropic coupling constant was negative and the parallel component of the dipolar coupling 2B are negative (-125, -233 ,212 and -178.1 G). These results can only occur for an orbital involving the d_{x2-y2} atomic orbital on copper. The value for 2B is quite normal for copper(Il) complexes[46]. The $|A_{iso}|$ value was relatively small. The 2B value divided by 2B° (The calculated dipolar coupling for unit occupancy of d_{x2-y2} (-235.11 G), using equation (10) suggests all orbital population close to 53-99.1 % d-orbital spin density, clearly the orbital of the unpaired electron is d_{x2-y2}[47]. Manganese(II**)** complex **(2)** showed isotropic type with g_{iso} = 2.02, indicating octahedral structure[37].

Thermal analyses (DTA and TGA): Since the IR spectra indicated the presence of water molecules, thermal analyses (DTA and TGA) were carried out to certain their nature. The thermal curves in the temperature 27-600° C range for complexes (**6**), (**9**), (**10**), and (**12**) are thermally stable up to 45 °C. Broken of hydrogen bonding occurs as endothermic peak within the temperature 45-50 °C as shown in (Table 5). Dehydration is characterized by endothermic peaks within the

temperature 55-65°C range, corresponding to the loss of hydrated water molecules.The elimination of coordinated water molecules occurred in 120-130°C range accompanied by endothermic peaks[49,50]

The TGA and DTA thermogram of Ni(II) complex (**6**) showed that, the complexe decomposed in six step. The first occurred at 45°C with no weight loss as endothermic peak, may be due to break of hydrogen bondings. The second step occured at 55°C with 6.72 % weight loss (Calc. 6.52%) as endothermic peak which could be due to the elimination of three hydrated water molecules.

The decomposition step which occurred at 120°C with 7.01% weight loss (Calc. 6.9%) could be due to the elimination of two coordinated H_2O. The TGA curve displayed another thermal decomposition at 230°C with 34.2% weight loss (Calc. 34.0%), which could be due to the loss of four coordinated acetate groups. The complex showed an exothermic peak observed at 350°C was due its melting point. Finally, exothermic peaks appeared at 405, 450, 485, 565 and 580 °C corresponding to oxidative thermal decomposition which proceeded slowly with leaving 2NiO with 32.8% weight loss (Calc. 32.6%)[51]. The TG and DTA thermogramof Cu(II) Complex (**7**) shows endothermic peak at 125°C with 5.6% weight loss (Calc. 5.5%) were assigned to two coordinated water molecules. The endothermic peak observed at 160°C with 24.1% weight loss (Calc. 23.3%), could be due to the elimination of four chloride ions. Another exothermic peak observed at 355 with no weight loss may be due to its melting point. Finally, the complex shows exothermic peaks at decomposition which proceeds slowly with final residue, assigned to CuO[52]. The TGA and DTA thermogramof Zn(II) complex (**12**) shows endothermic peak at 50°C, due to break of hydrogen bonding. Another endothermic peak appeared at 120°C with 10.4% weight loss (Calc. 10.36%), due to loss of two coordinated water molecules. The complex displayed another exothermic peak at 325°C may be assigned to its melting point. Oxidative thermal decomposition occurs in 450, 500, 550, 570 and 590°C with 34.8% weight loss (Calc. 34.5%) exothermic peaks, leaving 2ZnO [51].

Transmission electron microscope characterization (TEM): The average diameter of the ligand and the complex particles Co(II), complex **(4)** was determined to be 39.25 ± 3.51 nm and 23.24 ± 2.45 nm respectively. All complexes are present in nano size particles i.e., their particles present in a diameter between 1 and 100 nm in size. The complex **(4)** and the ligand show sign with ratio that exhibit new or enhanced size-dependent properties compared with larger particles of the same material with many advantages such as:

Increased bioavailability, dose proportionality, decreased toxicity, smaller dosage form (i.e., smaller tablet), stable dosage forms of drugs which are either unstable or have unacceptably low bioavailability in non-nanoparticulate dosage forms, increased active agent surface area results in a faster dissolution of the active agent in an aqueous environment, such as the human body, faster dissolution generally equates with greater bioavailability, smaller drug doses, less toxicity and reduction in fed/fasted variability.

Table 4. ESR data for some metal (II) complexes:-

No.	$g_{\parallel}$	$g_{\perp}$	g_{iso}[a]	$A_{\parallel}$ (G)	$A_{\perp}$ (G)	A_{iso}[b] (G)	G [c]	ΔE_{xy}	ΔE_{xz}	$K_{\perp}^2$	$K_{\parallel}^2$	K	K^2	$g_{\parallel}/A_{\parallel}$	α^2	$ß^2$	$ß_1^2$	-2B	a_d^2(%)
(2)	-	-	2.02	-	-	-	-	-	-	-	-	-	-	-	-	-	-	-	-
(3)	2.15	2.5	-	100	12.5	-	-	-	-	-	-	-	-	-	-	-	-	-	-
(4)	2.19	2.5	-	90	10	-	-	-	-	-	-	-	-	-	-	-	-	-	-
(5)	-	-	2.04	-	-	-	-	-	-	-	-	-	-	-	-	-	-	-	-
(7)	-	-	2.15	-	-	-	-	-	-	-	-	-	-	-	-	-	-	-	-
(8)	2.21	2.09	2.13	120	15	50	4.6	17857	21052	1.11	0.56	0.92	0.84	149.2	0.62	1.79	0.9	125	53
(9)	2.18	2.05	2.09	120	15	50	3.6	17182	21645	0.62	0.46	0.75	0.57	181.6	0.57	1.08	0.8	233	99.1
(10)	2.20	2.07	2.11	100	10	40	2.86	17271	21834	0.89	0.51	0.87	0.76	220	0.55	1.6	0.93	212	90.3
(11)	2.16	2.04	2.08	90	15	40	4.0	17699	22222	0.51	0.42	0.65	0.48	222	0.45	1.13	0.93	178.1	76

$g_{iso} = (2g_{\perp} + g_{\parallel})/3$, b) $A_{iso} = (2A_{\perp} + A_{\parallel})/3$, c) $G = (g_{\parallel} - 2)/(g_{\perp} - 2)$

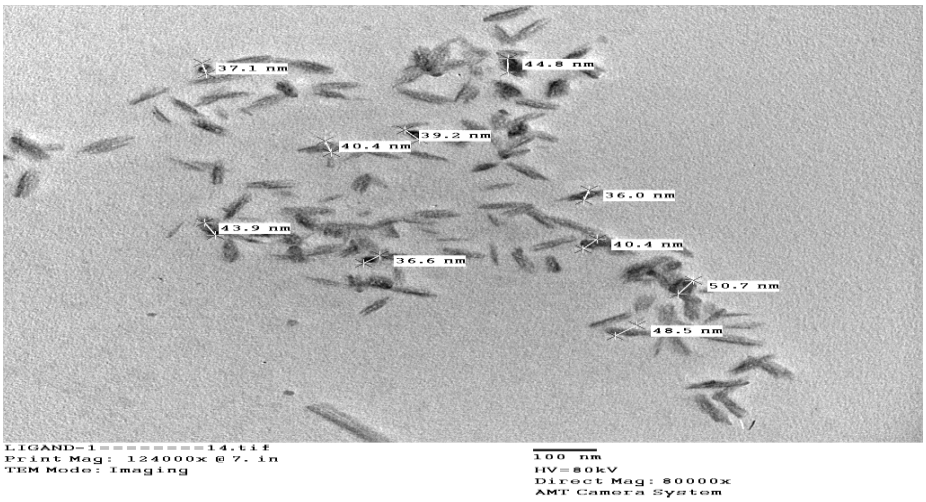

Fig. 3.TEM images for ligand nanoparticles

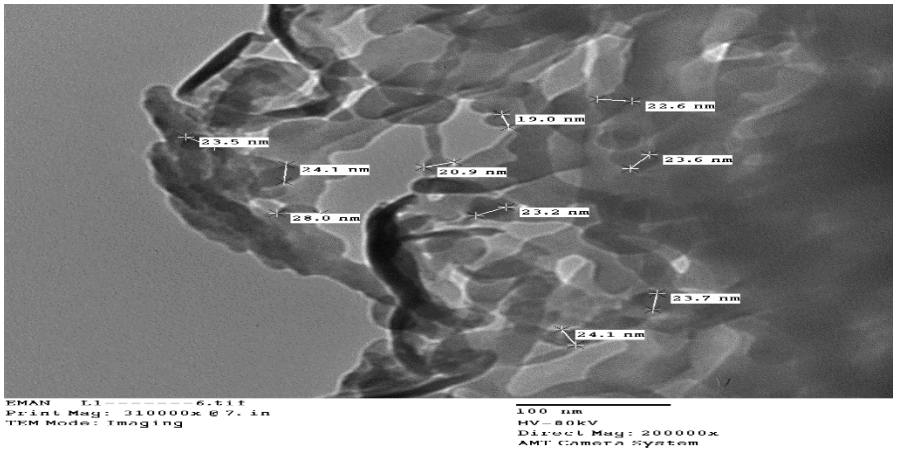

Fig. 4. TEM images for Co(II) complex **(4)** nanoparticles

Cytotoxic Activity: Chemotherapeutic studies: The biological activity of the ligand (**1**) and its metal complexes (**4**), (**8**), and (**12**) were evaluated against MCF-7 cell line. In this study, we try to know the chemotherapeutic activity of the tested complexes by comparing them with the standard drug (IMURAN (azathioprine)). The treatment of the different complexes in DMSO showed similar effect in the tumoral cell line used as it was previously reported[53]. The solvent dimethyl sulphoxide (DMSO) shows no effect in cell growth. The ligand (**1**) shows a weak inhibition effect at ranges of concentrations used, however, the complexes showed better effect against MCF-7 cell line. The obtained data indicate the surviving fraction ratio against MCF-7 cell line increasing with the decrease of the concentration in the range of the tested concentrations. Also, the Co(II) complex (**4**) shows the highest potency of inhibition at 50 µg/ml against MCF-7 cell lines, compared with the standard drug[72]. Cytotoxicity results indicated that the tested complexes (**4), (8)** and **(12)** (IC_{50} = 23.42–178.54 μM) demonstrated potent cytotoxicity against MCF-7 cancer cell as shown at Figures 5-9.

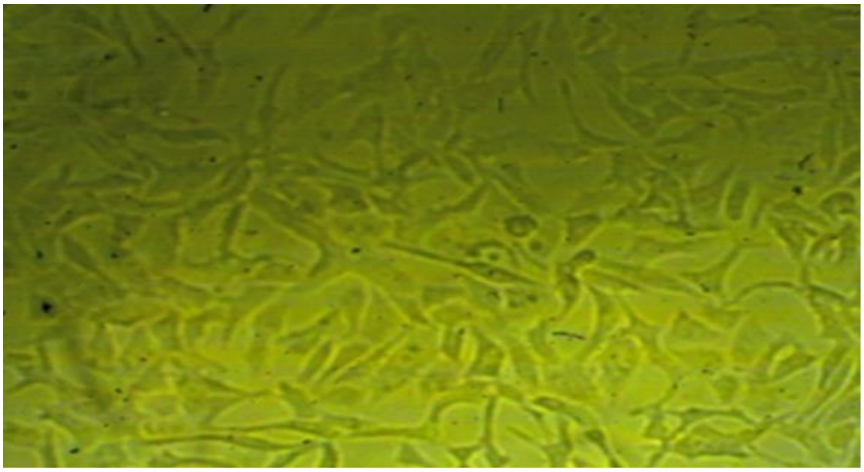

Fig. 5. Positive control of MCF-7 cells

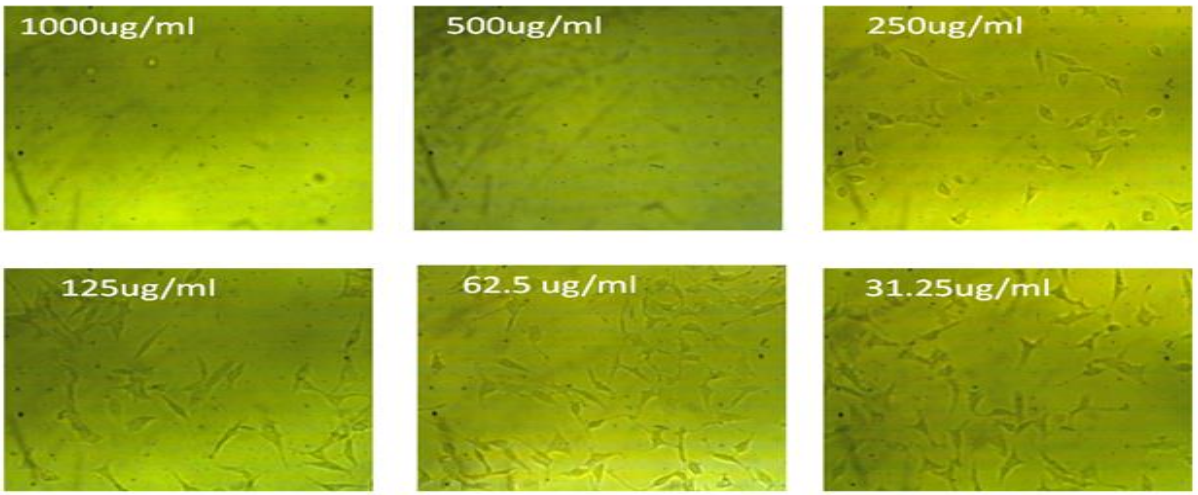

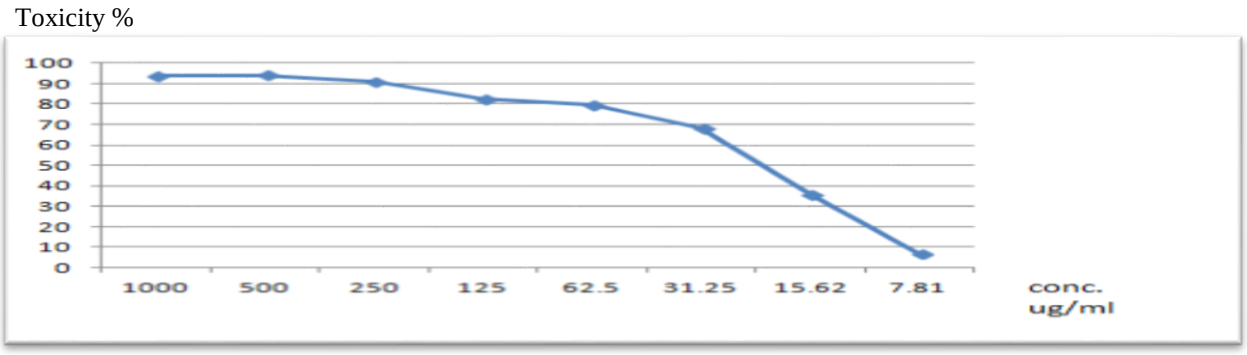

Fig. 6. Effect of ligand (1) on MCF-7 cells at different concentration

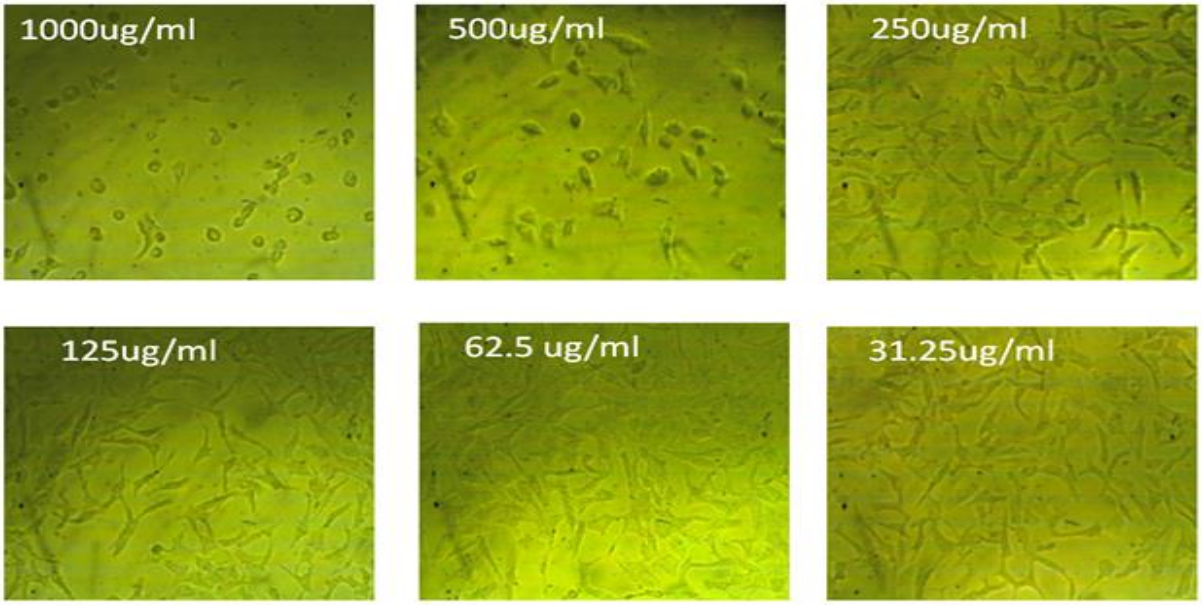

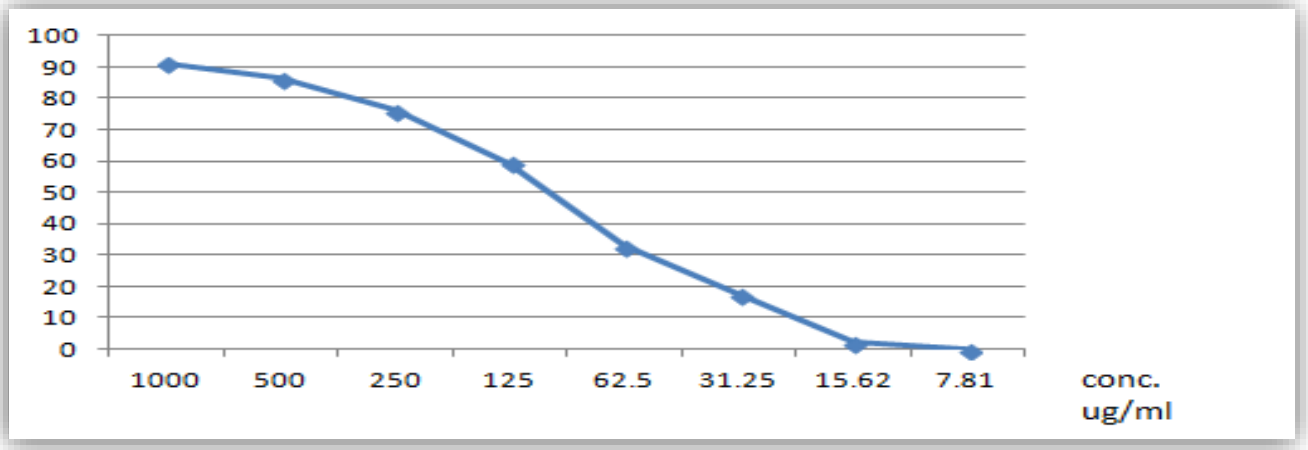

Fig. 7. Effect of complex (4) on MCF-7 cells at different concentration

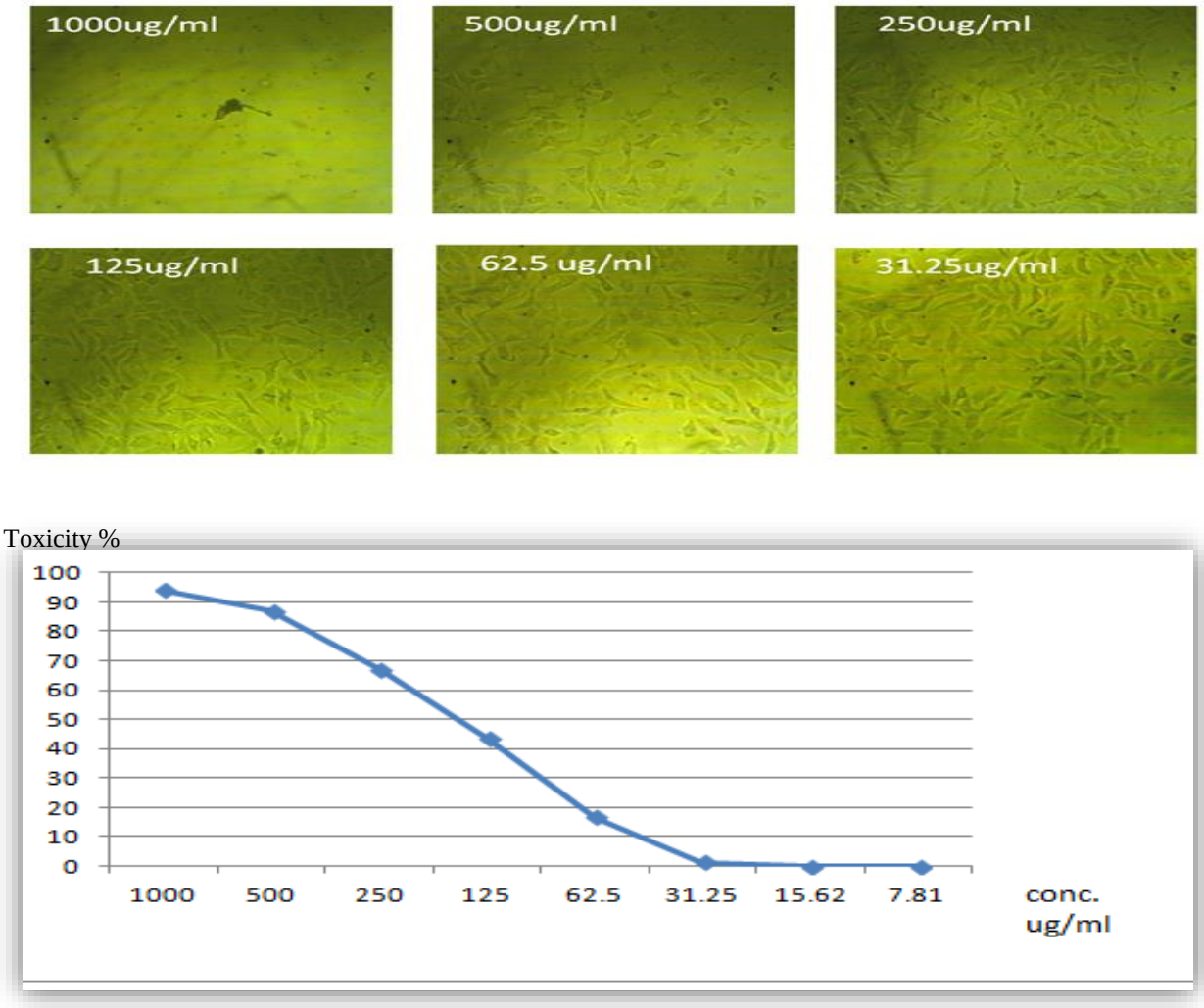

Fig. 8. Effect of complex (8) on MCF-7 cells at different concentration

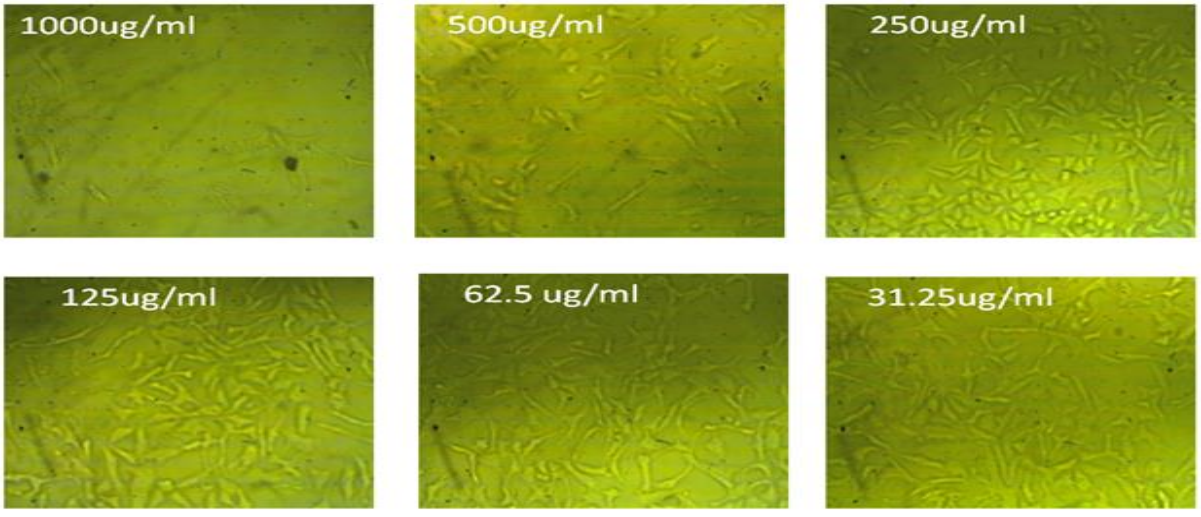

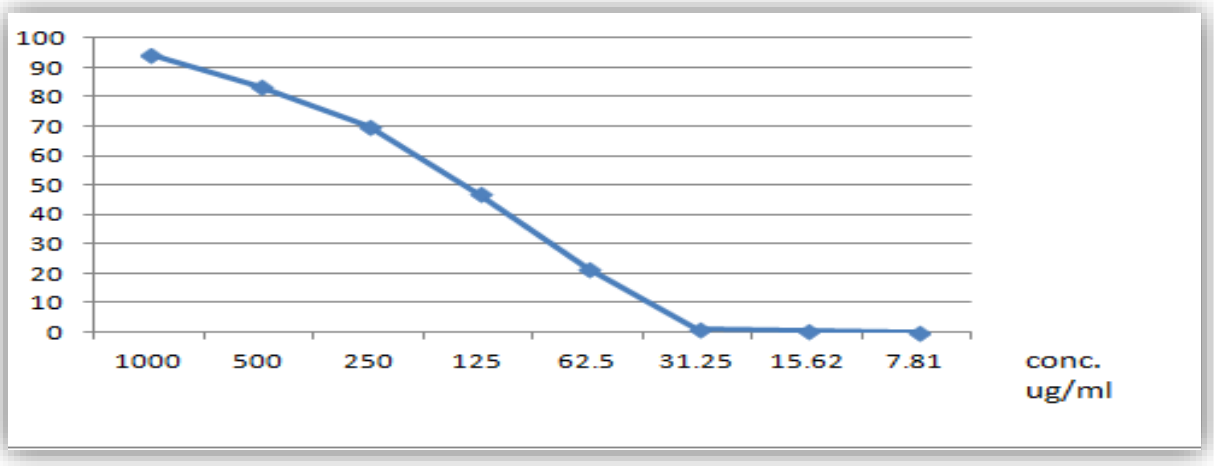

Fig. 9. Effect of complex (12) on MCF-7 cells at different concentration

From histograms we found that:-

(1) Decrease in the number of available cells.

(2) Most of the remaining observed degeneration changes in the form of the irregularly cell membrane opaque and not well formed chromatin regulated of swelling cytoplasm, other showed optimistic change in the formed of shrunken cells and increase eosinophilia cells , and picknitoic nucleus.

Conclusion

In the present study, new metal(II) complexes of N-(2-((E) (2hydroxybenzylidene)amino) phenyl)-2-((E)-((6-hydroxycyclohexa-1,5-dien-1-yl)methylene) amino) butanamide were prepared. Structural and spectroscopic properties revealed that, the ligand adopted a triradentate or hexadentate ligand fashion; on the other hand, the metal complexes adopted a tetragonal distorted octahedral geometry around metal ions. All the complexes are non-electrolytic in nature as suggested by molar conductance measurements. The ligand coordinated to the central metal ion forming five six membered rings including the metal ions. The antitumor activities of the ligand as well as some of its metal complexes were assessed that ,the toxicity of both ligand and some of its metal complexes was found to be concentration dependent, the cell viability decreased with increasing the concentration of complexes.

References

1. B. S. Tovrog, D. J. kitko and R. S. Dragom, *J. Am. Chem. Soc.*, 1976, 98, 5144.
2. N. Batra and J. Devi, *J. Chem. Pharma. Res.*, 2015, 7, 183.
3. Y. Xiao, C. Bi, Y. Fan, S. Liu, X. Zhang, D. Zhang, Y. Wang and R. Zhu, *J. Coord. Chem.*,2009, 62, 3029.
4. E. I. Solomon, M. D. Lowery, "Electronic structure contributions to function in bioinorganic chemistry" *Science*,1993, 259(5101), 1575–1581.
5. 5. M. Tümer, E. Akgün, S. Toroglu, A. Kayraldız and L. Dönbak, *J. Coord. Chem., 2008*, 61(18), 2935–2949.
6. A. Gölcü, M. Tümer, H. Demirelli and R. A. Wheatley, *Inorg. Chim. Acta*, 2005, 358, 785–1797.
7. C. Gerdemann, C. Eicken and B. Krebs, *Accounts Chem. Res*., 2002, 35, 183–191.
8. E. Alessio, *Bioinorganic Medicinal Chemistry*, *Weinheim*, *Wiley-Vch*, 2011.
9. M. Gielen and E. R. T Tiekink, Metallotherapeutic Drugs and Metal-based diagnostic agents, John Wiley and Sons Ltd., Chichester, 2005.
10. G. Svehla, Vogel's Textbook of macro and semimicro qualitative inorganic analysis, Longman London, 1979.
11. F. J. Welcher, analytical uses of ethylene diaminetetraacetic acid, 1958.
12. A. A. Vogel, Text Book of Quantitative Inorganic Analysis, 1978, ELBS, London.
13. B. Figgis, J. Lewis and R. Wilkins, Modern coordination chemistry, *Interscience*, New York, 1960, 403.
14. V. Vichai and K. Kirtikara, *Nature Protocols*, 2006, 1112 – 1116.
15. A. S. El-Tabl, M. M. Abd El-Waheed, M. A.Wahba and N. A. AbouEl-Fadl, *Bioinorg. Chem. Appl.*,2015, 1-14.

16. W. Geary, *J. Coord. Rev.*,1971, 7, 81-122.
17. A. S. El-Tabl, M. M. E. Shakdofa, A. M. A El-Seidy and A.N.Al-Hakimi, *J. koarin. Chem. Soc.*, 2011, 55, 19.
18. A. S. El-Tabl, F. A. El-Saied and A. N. Al-Hakim, *Trans. Met. Chem.*, 2007, 32, 689.
19. A. S. El-Tabl, M. M. E. Shakdofa, A. M. A. El-Seidy, *Korean J. Chem. Soc.*, 2011, 55, 603.
20. M. M. Aly, S. M. Imam, *Montash Chem.*, 1995, 126, 137.
21. A.S. El-Tabl, T. L. Kashar, R.M. El-Bahnasay, A. El-Mohsef, *Polish J.Chem*., 1999, 73, 245.
22. A. S. El-Tabl, *Trans. Met. Chem., 2002*, 27, 166.
23. Nakatamato, Infrared Spectra of Inorganic and Coordination compounds, second ed., Wiley, New York, 1971.
24. H. A. Kuska, M. T. Rogers, in: A. E. Martell (Ed), Coordination Chemistry, vol. 92, Van Nos-tradReihoid Co., New York, 1971.
25. A. S. El-Tabl, *Trans. Met Chem.*, 2002, 27, 166.
26. A. S. El-Tabl, *J. Chem. Res.*, 2002, 529-531.
27. R. M. El-Bahnasawy, A. S. El-Tabl, E. El-Sheroafy, T. I. Kashar and Y. M. Issa, *Polish J. Chem.*1995, 73.
28. K. B. Gudasi, S. A. Patel, R. S. Vadvavi, R. V. Shenoy and M. Nethayi, *Trans. Met. Chem.*, 2006, 31, 580-585.
29. A. S. El-Tabl, F. A. El- Said, A. N. Al-Hakim, *Trans. Met. Chem*., 2007, 67, 265.
30. N. A. Al-Hakimi, M. M. E. Shakdofa, A. M. A. El-Saidy and A. S. El-Tabl, *J. Korean Chem. Soc.*, 2011, 55, 418.
31. A. S. El-Tabl, S . A, El-Enein, *J. Coord. Chem.*,2004, 57, 281.
32. S. A. Sallam, A. S. Orabi, B. A. El-Sheraty and A. Lentz, *Trans. Met. Chem.*2002, 27, 447.
33. G. C. Chinvmia, D. G. Phillips and A. D. Rae, *Inorg. Chim. Acta*, 1995, 238, 197-201.
34. A. S. El-Tabl, *Bull. Korean Chem.Soc.*, 2004, 25, 1-6.
35. A. S. El-Tabl, M. M. E. Shakdofa and A. M. A. El-Seidy, *Korean J. Chem. Soc.*, 2011, 55, 603.
36. H. A. El-Boraey and A. S. El-Tabl, *Polish J. Chem.*,2003, 77, 1759-1775.
37. A. S. El-Tabl, *Trans. Met. Chem.*, 1998, 23, 63.
38. I. M. Procter, B. J. Hathaway and P. N. Nicholls, *J. Chem. Soc. A*, 1969, 1678-1684.
39. D. E. Nikles, M. J. Powers and F. L. Urbach, *Inorg. Chem.*, 1983, 22, 3210.
40. R. K. Ray, *J. Inorg. Chim. Acta*, 1990, 174, 257.
41. D. W. Smith, *J. Chem. Soc. A*, 1970, 22, 3108.
42. A. S. El-Tabl, *J. Chem. Res.*, 2004, 19.
43. D. Kivelson and R. Neiman, *J. Chem. Phys.*, 1961,35, 149.
44. M. M. Bhadbhade and D. J. Srinivas, *Inorg. Chem.*, 1993, 32, 2458.
45. M. C. R. Symons, "Chemical and Biological Aspects of Electron Spin Resonance, Van Nostrand Reinhold", Wokingham 1979.
46. A. S. El-Tabl, M. M. E. Shakdofa and A. M. A. El-Seidy, *J. Korean Chem. Soc.*, 2011, 55, 603-611
47. A. N. Alhakimi, A. S. El-Tabl and M. M. E. Shakdofa, *J. Chem Res.*, 2011, 770-774.
48. C. Natarajan, P. Shanthi, P. Athappan and R. Mvrvgesan, *Trans. Met. Chem.*,1992, 17, 39.
49. A. S. El-Tabl and S. M. Imam, *Trans. Met.Chem.*, 1997, 22, 259.
50. M. Gaber and M. M. Ayad, Thermochim, *Acta*, 1991, 176, 21-29.
51. A. S. El-Tabl and M. M. Abou-Sekkina, *polish J. Chem.*,1999, 73, 1937.
52. A. S. El-Tabl, M. M. Abou-Sekkina, *Polish J.Chem*., 1999, 73, 937-1945.
53. N. A. Illan- Cabeza, A. R. Garcia-Garcia, M. N. Moreno-carretero, J. M. Martin-Martos and M. J. J. Ramirez-exposito, *Inorg. Biochem*., 2005, 99, 1637.